Supporting Information for

Benchmarking of commercial Cu catalysts in CO_2 electroreduction using gas-diffusion type microfluidic flow electrolyzer

Haocheng Xiong[1, 2], Jing Li[1], Donghuan Wu[1], Bingjun Xu[2,*] and Qi Lu[1,*]

[1]State Key Laboratory of Chemical Engineering, Department of Chemical Engineering, Tsinghua University, Beijing 100084, China

[2]College of Chemistry and Molecular Engineering, Peking University, Beijing 100871, China

*Corresponding authors: b_xu@pku.edu.cn, luqicheme@mail.tsinghua.edu.cn

EXPERIMENTAL SECTION

Materials. Carbon dioxide (CO_2, 99.999%), Carbon monoxide (CO, 99.999%) and Argon (Ar, 99.999%) were purchased from Air Liquide. Potassium hydroxide (semiconductor grade, 99.99% trace metals basis) and Potassium chloride (99.99% trace metals basis) were purchased from Sigma-Aldrich. IrO_2 powder (99.99% trace metals basis) was purchased from Alfa Aesar. Milli-Q water (18.2 MΩ cm) was used to prepare all the electrolytes. Nano Particle Cu (NP Cu, nanopowder, 25 nm particle size (TEM)) was purchased from Sigma-Aldrich, Cu powder in spherical form (Sph Cu, 99.9%) was purchased from Macklin, and CuO powder (30-50nm APS Powder) was purchased from Alfa Aesar. Carbon paper (Sigracet 29BC) and anion-exchange membrane (Selemion AMV AGC Inc.) were purchased from SINERO TECHNOLOGY. Nafion solution (5 wt %) was purchased from Sigma-Aldrich.

Physical Characterizations. The powder X-ray diffraction patterns were conducted on an automated powder X-ray diffractometer (Rigaku MiniFlex 600 with Cu Kα radiation). The morphology of the Cu catalyst was characterized by field emission scanning electron microscope (Merlin FE-SEM, Zeiss). X-ray photoelectron spectroscopy measurements were conducted on an AXIS Supra and CasaXPS software (Casa Software Ltd., UK) was used for data analysis.

Electrode preparation. To prepare the cathode electrode, an ink containing a mixture of Nafion, ethanol and catalysts was airbrushed (using Ar gas as a carrier gas) on a carbon paper serving as substrate. After drying under vacuum for 12 hours, an 1.2 × 2.2 cm^2 electrode was cut and assembled into a custom-designed gas-diffusion type

microfluidic flow cell.

Electrocatalytic Measurements. The electrochemical measurements were conducted in a three-compartment microfluidic flow cell with a channel dimension of 2 cm × 0.5 cm × 0.2 cm. A piece of anion-exchange membrane (Selemion AMV AGC Inc.) separated the working and counter compartments. The IrO_2 coated Ti foam with a catalysts loading of 1.0 mg/cm^2 was used as the counter electrode, and a leak-free Ag/AgCl (3.4 M KCl, Innovative Instruments Inc.) was used as the reference electrode. Gas was fed into the cathode chamber at a flow rate of 20.0 cm^3/min using a mass flow controller (MKS Instruments Inc.) and calibrated through an Agilent ADM flow meter. The gas-phase pressure was regulated using a backpressure controller (Cole-Parmer). The flow rate of electrolyte was set to be at 5 mL/min via a peristaltic pump (Kamoer). The catalysts were pre-treated by reducing at -5 mA/cm^2 for 300 s before measurements. Chronopotentiometry experiments (Fig. 2, Fig. 3a and Fig. 4) were conducted to benchmark the CO_2 and CO electroreduction performance at fixed current densities. The measured potential was manually IR corrected after the electrolysis. For chronoamperometry measurement (Fig. 3b), the equivalent resistance between GDL and reference electrode was measured after the pre-treatment, and then was corrected to arrive an electrode potential of -1.52 V (±50 mV). Gas products were quantified by a gas chromatograph (Agilent 7890) and liquid products were determined by a Bruker AVIII 400 MHz NMR spectrometer.[1] A Gamry Reference 1000+ Potentiostat was used for electrochemical measurements.

Electrochemically Active Surface Area Measurements. The ECSAs of electrodes

were determined by measuring the electrochemical double-layer capacitance (CDL) in an H-type cell.[2] All electrodes were electrochemically pre-treated at -5 mA/cm^2 for 300s in 0.1 M KOH before ECSA measurements. Cyclic voltammetry was conducted on each electrode at various scan rates (i.e., 20, 40, 60, 80, and 100 mV/s) at an Ar atmosphere in 0.1 M $HClO_4$. The potential region of no Faradaic current ranged from −300 to −150 mV vs Ag/AgCl (3 M KCl). The observed current was plotted versus the scan rate to obtain the capacitance of different electrodes (Fig. S6).

Table S1. Comparison of total current density and C_{2+} products Faradaic efficiencies (FE) of different catalysts for CO_2 electroreduction operated at commercially relevant current densities (> 100 mA/cm^2). The SHE reference scale was converted to the RHE reference scale as follows: E (vs RHE) = E (vs SHE) + 0.0591 V × pH.

Catalyst	Feed-stock	Electrolyte	Potential (V_{RHE})	FE_{C2+} (%)	Total Current Density (mA/cm^2)	Reference
NP Cu (0.2 mg/cm^2)	**CO_2**	**1 M KOH**	**-0.74**	**79.3**	**300**	**This work**
NP Cu (1.4 mg/cm^2)	**CO_2**	**1 M KOH**	**-0.69**	**70.2**	**957**	**This work**
OD Cu (0.4 mg/cm^2)	**CO_2**	**1 M KOH**	**-0.58**	**71.3**	**200**	**This work**
Sph Cu (1.2 mg/cm^2)	**CO_2**	**1 M KOH**	**-0.71**	**69.7**	**200**	**This work**
Fragmented Cu	CO_2	7 M KOH	-0.69	77.8	300	[3]
Boron-Doped CuO	CO_2	1 M KOH	-0.62	62.1	139	[4]
Cu_4O_3-rich catalyst	CO_2	0.5 M Cs_2SO_4	-0.64	61.7	300	[5]
Hierarchical Cu_2O	CO_2	1 M KOH	N.A.	71.1	200	[6]
CuDAT-wire	CO_2	1 M KOH	−0.69	70.9	254	[7]
$Ce(OH)_x$/Cu/PTFE	CO_2	1 M KOH	-0.7	80.3	297	[8]
$Cu_{1.0}/ZnO_{0.30}$	CO_2	1 M KOH	-0.72	70	700	[9]
Cu_3N_x-50-μA	CO_2	1 M KOH	-1.15	81.7	307	[10]
CuPb-0.7/C	CO_2	1 M KOH	N.A.	81.6	300	[11]
$Cu_2P_2O_7$	CO_2	1 M KOH	N.A.	73.6	350	[12]
Cu-TABQ	CO_2	1 M KOH	-1.17	63	423	[13]
Au-Cu Janus	CO_2	3 M KOH	-0.75	67	290	[14]

Cu HoMSs	CO_2	0.5 M $KHCO_3$	-0.91	77	513.7	[15]
AgI-CuO	CO_2	1 M $KHCO_3$	-1.15	63.2	200	[16]
F-Cu	CO_2	1 M KOH	-1.17	70.4	450	[17]
N_2SN-Ag-Cu	CO_2	0.1 M $KHCO_3$	N.A.	80	261	[18]
Sputtered Cu	CO_2	1 M KOH	-0.6	72	250	[19]
	CO_2	0.5 M $KHCO_3$	-0.94	68	250	

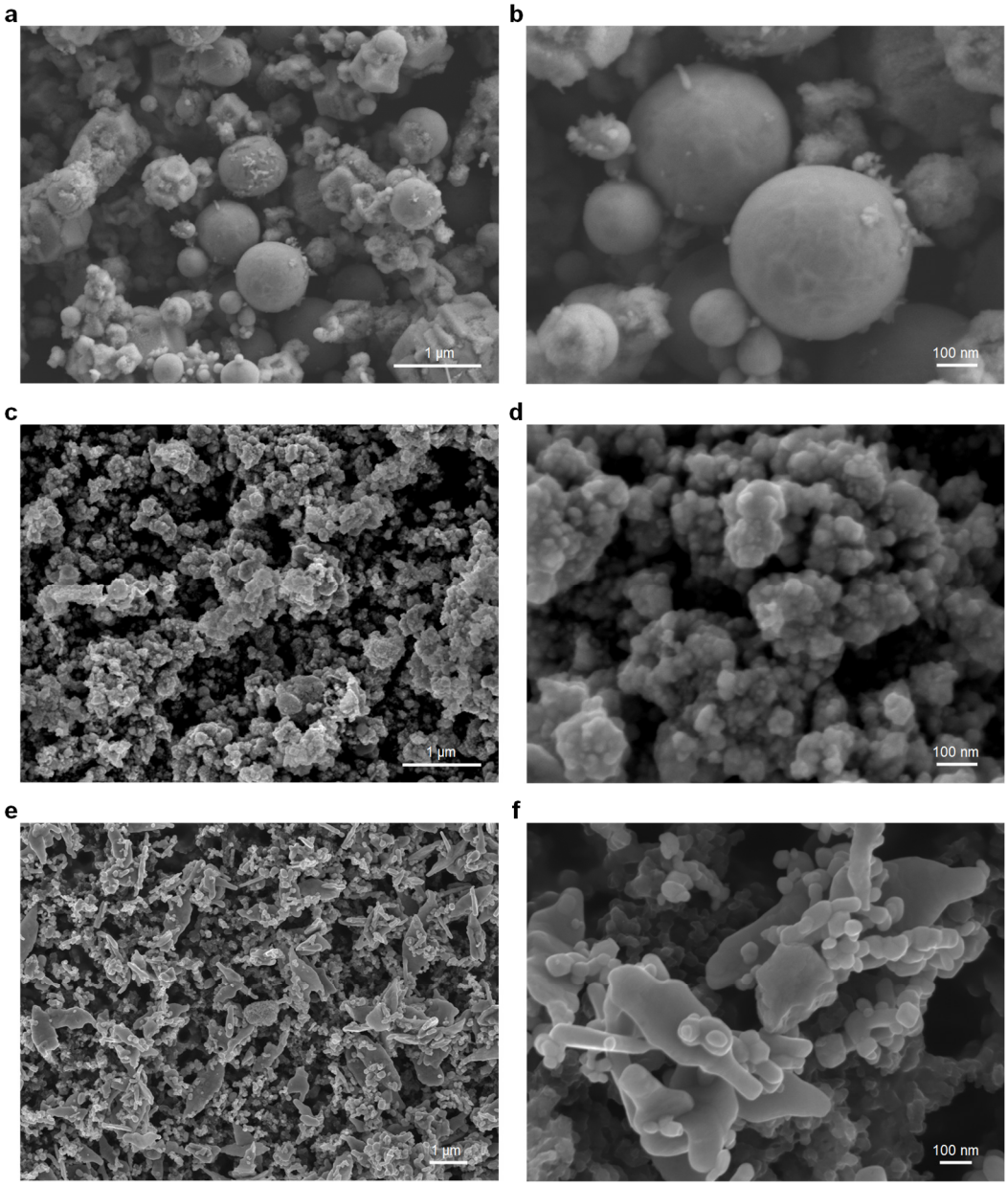

Fig. S1. SEM images of Sph Cu (**a**, **b**), NP Cu (**c**, **d**) and CuO (**e**, **f**).

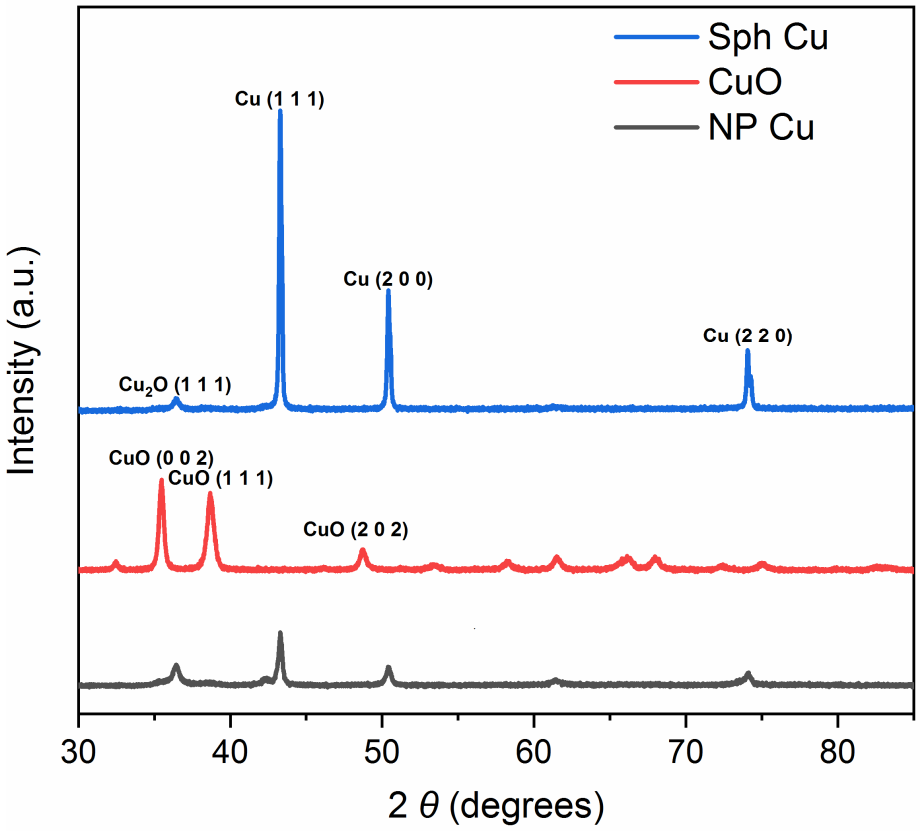

Fig. S2. Powder X-ray diffraction patterns of Sph Cu, CuO and NP Cu (Cu PDF #04-0836 and CuO PDF #45-0937).

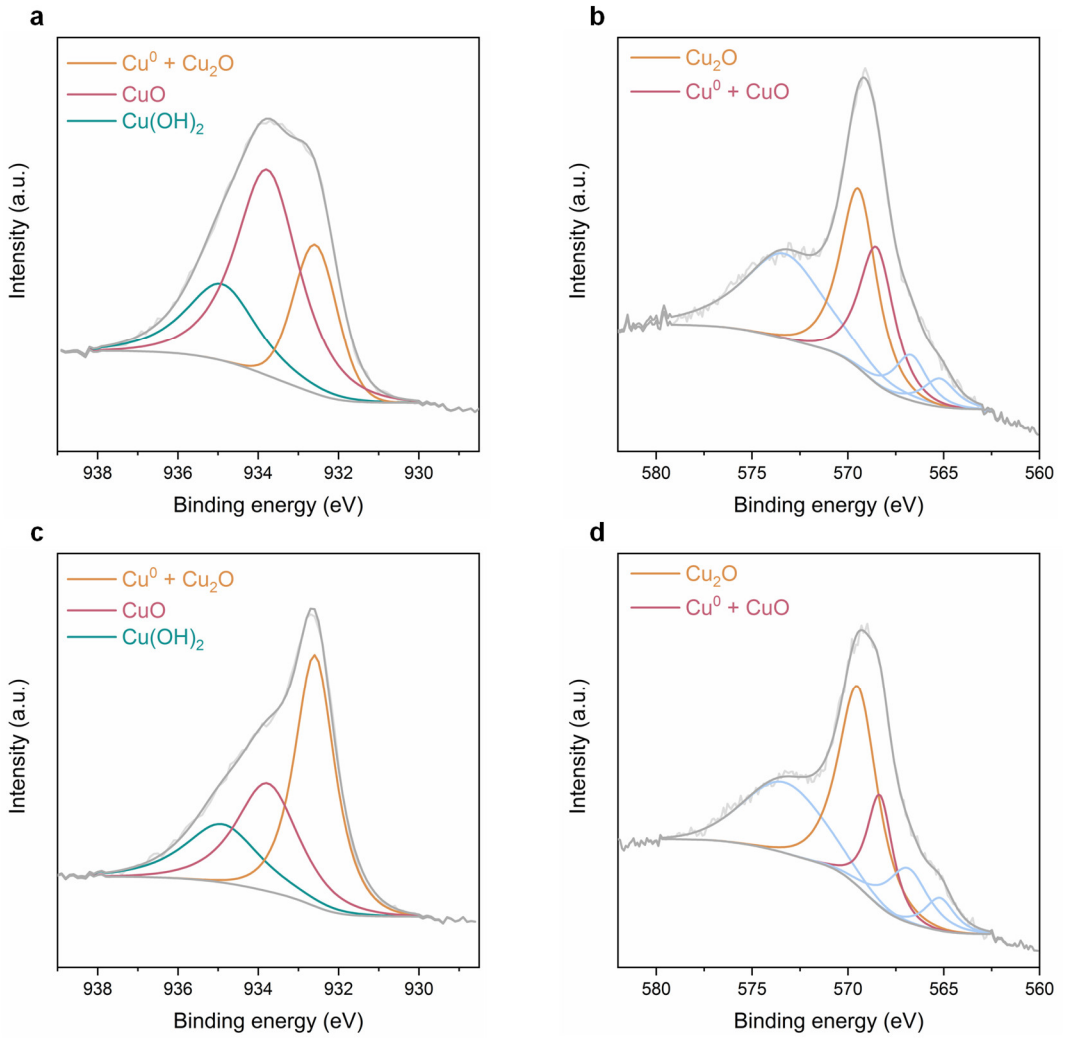

Fig. S3. X-ray photoelectron spectroscopy characterizations for NP Cu and Sph Cu. (**a**) NP Cu 2p3/2 spectrum. (**b**) NP Cu LMM spectrum. (**c**) Sph Cu 2p3/2 spectrum. (**d**) Sph Cu LMM spectrum.

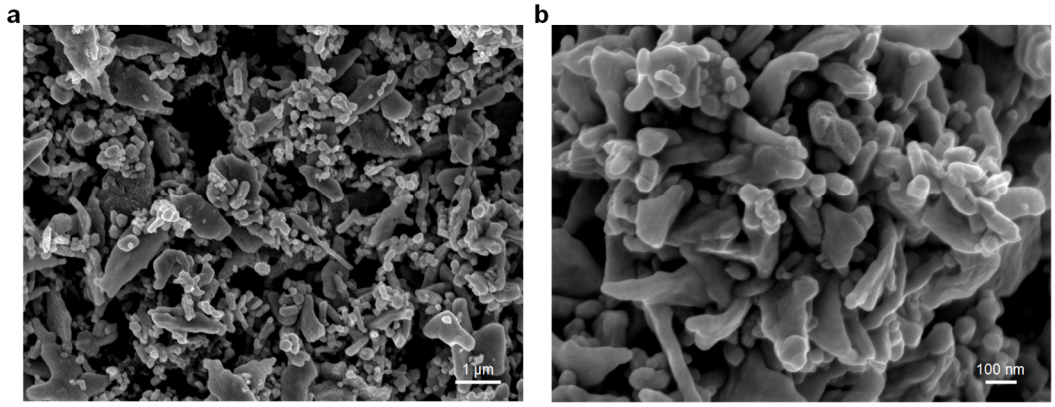

Fig. S4. SEM images of OD Cu on carbon paper at different magnifications. CuO electrodes were treated with a pre-electroreduction at a constant current density of -5 mA/cm^2 for 300 s to convert CuO into OD Cu.

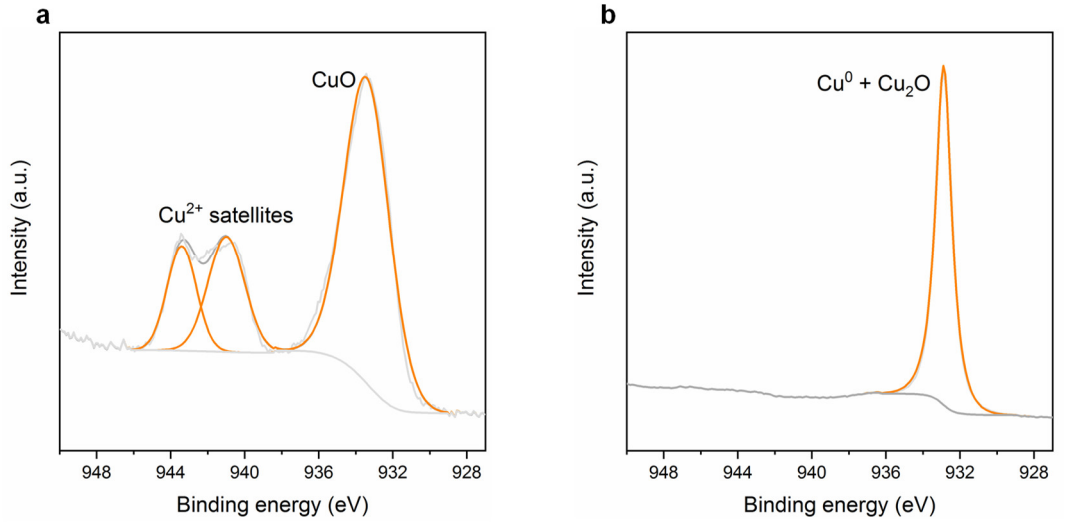

Fig. S5. X-ray photoelectron spectroscopy of 2p3/2 spectra for CuO (**a**) and OD Cu (**b**).

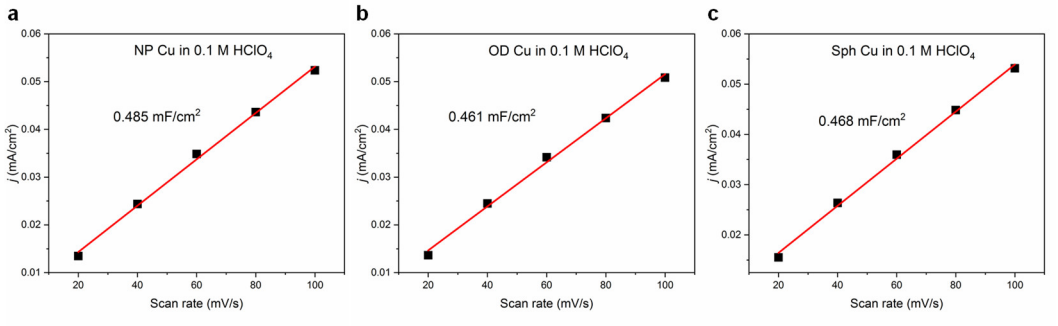

Fig. S6. Measured double layer charging current vs scan rate for NP Cu (**a**), OD Cu (**b**) and Sph Cu (**c**).

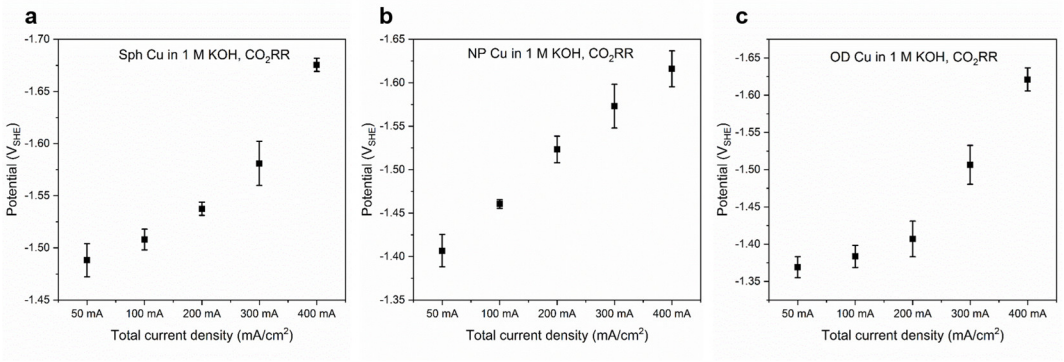

Fig. S7. Potential vs. total current densities for CO_2RR over Sph Cu (**a**), NP Cu (**b**) and OD Cu (**c**) in 1 M KOH. Error bars represent the standard deviation from at least three independent measurements.

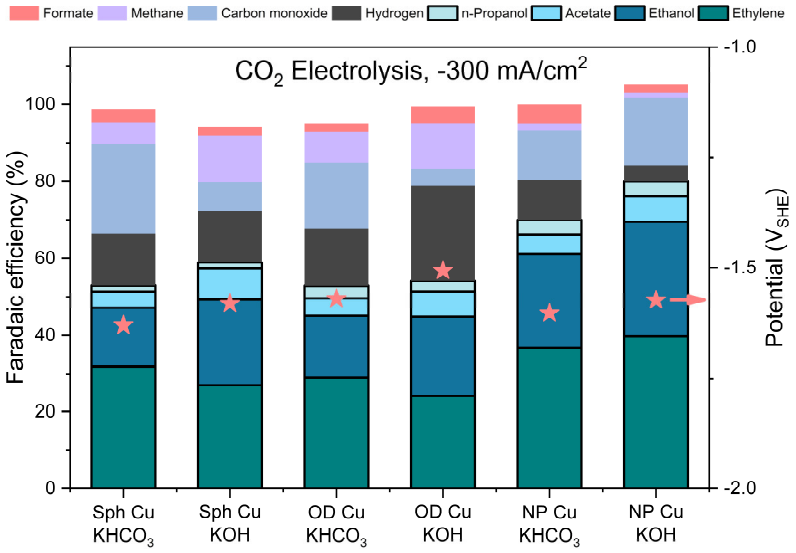

Fig. S8. Comparison of CO_2RR performance of commercial Cu catalysts in 1 M $KHCO_3$ and 1 M KOH at fixed current density of 300 mA/cm^2.

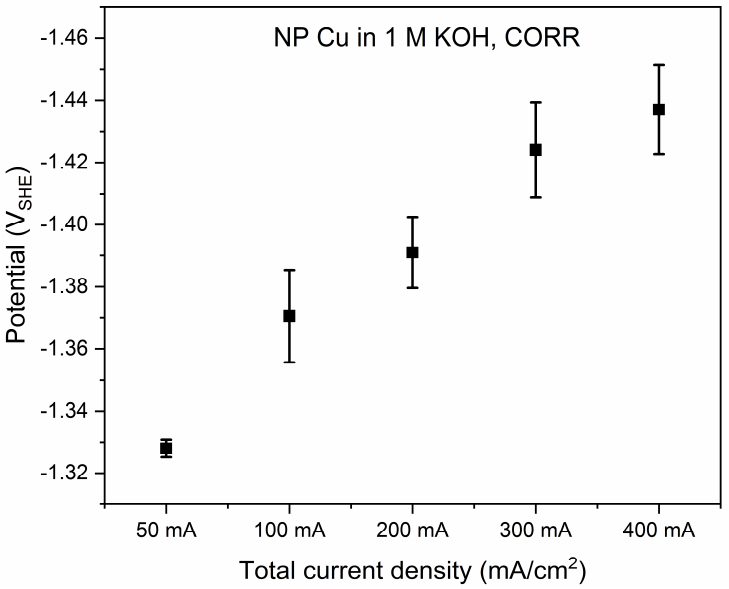

Fig. S9. Potential vs. total current densities for CORR over NP Cu in 1 M KOH. Error bars represent the standard deviation from at least three independent measurements.

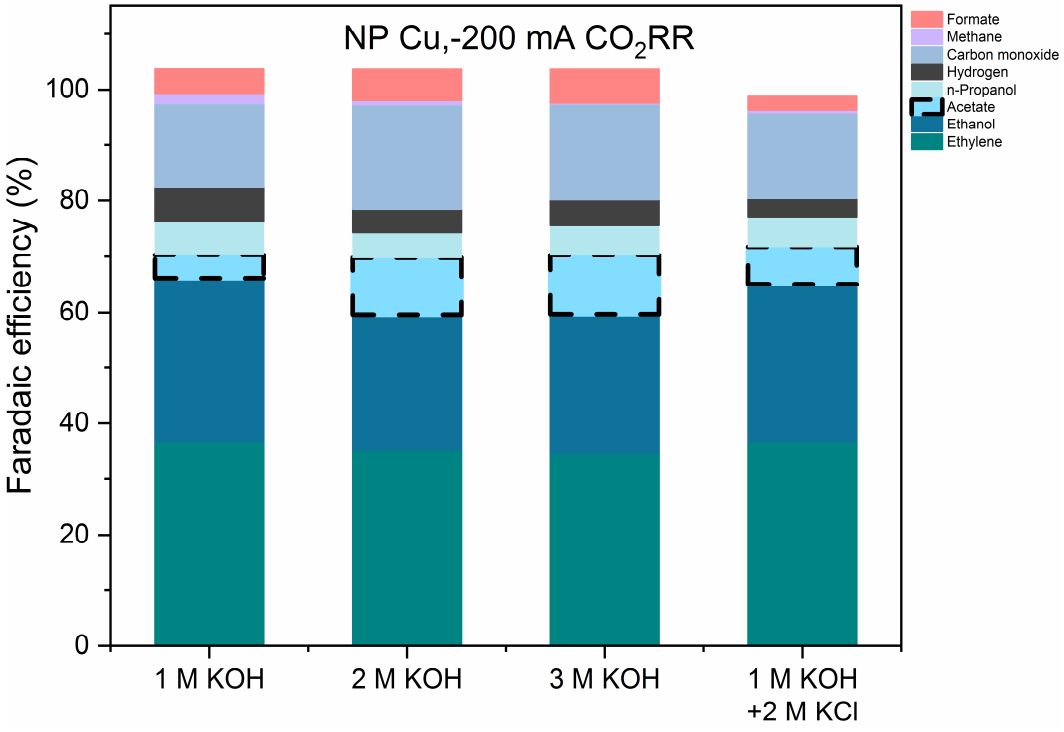

Fig. S10. CO_2 electroreduction at 200 mA/cm^2 over NP Cu in different electrolytes.

References

1 J. Li, K. Chang, H. Zhang, M. He, W. A. Goddard, J. G. Chen, M.-J. Cheng and Q. Lu, *ACS Catal.*, 2019, **9**, 4709-4718.
2 M. Jouny, W. Luc and F. Jiao, *Nat. Catal.*, 2018, **1**, 748-755.
3 K. Yao, J. Li, H. Wang, R. Lu, X. Yang, M. Luo, N. Wang, Z. Wang, C. Liu, T. Jing, S. Chen, E. Cortes, S. A. Maier, S. Zhang, T. Li, Y. Yu, Y. Liu, X. Kang and H. Liang, *J. Am. Chem. Soc.*, 2022, **144**, 14005-14011.
4 K. K. Patra, S. Park, H. Song, B. Kim, W. Kim and J. Oh, *ACS Appl. Energy Mater*, 2020, **3**, 11343-11349.
5 N. Martić, C. Reller, C. Macauley, M. Löffler, B. Schmid, D. Reinisch, E. Volkova, A. Maltenberger, A. Rucki, K. J. J. Mayrhofer and G. Schmid, *Adv. Energy Mat.*, 2019, **9**.
6 M. Jun, C. Kwak, S. Y. Lee, J. Joo, J. M. Kim, D. J. Im, M. K. Cho, H. Baik, Y. J. Hwang, H. Kim and K. Lee, *Small Methods*, 2022, **6**, e2200074.
7 T. T. H. Hoang, S. Verma, S. Ma, T. T. Fister, J. Timoshenko, A. I. Frenkel, P. J. A. Kenis and A. A. Gewirth, *J. Am. Chem. Soc.*, 2018, **140**, 5791-5797.
8 M. Luo, Z. Wang, Y. C. Li, J. Li, F. Li, Y. Lum, D. H. Nam, B. Chen, J. Wicks, A. Xu, T. Zhuang, W. R. Leow, X. Wang, C. T. Dinh, Y. Wang, Y. Wang, D. Sinton and E. H. Sargent, *Nat. Commun.*, 2019, **10**, 5814.
9 T. Zhang, Z. Li, J. Zhang and J. Wu, *J. Catal.*, 2020, **387**, 163-169.
10 C. Peng, G. Luo, Z. Xu, S. Yan, J. Zhang, M. Chen, L. Qian, W. Wei, Q. Han and G. Zheng, *Adv. Mater.*, 2021, **33**, e2103150.
11 P. Wang, H. Yang, Y. Xu, X. Huang, J. Wang, M. Zhong, T. Cheng and Q. Shao, *ACS Nano*, 2021, **15**, 1039-1047.
12 J. Sang, P. Wei, T. Liu, H. Lv, X. Ni, D. Gao, J. Zhang, H. Li, Y. Zang, F. Yang, Z. Liu, G. Wang and X. Bao, *Angew. Chem. Int. Ed. Engl.*, 2022, **61**, e202114238.
13 F. Zhang, P. Wang, R. Zhao, Y. Wang, J. Wang, B. Han and Z. Liu, *ChemSusChem*, 2022, **15**, e202201267.
14 Y. Zheng, J. Zhang, Z. Ma, G. Zhang, H. Zhang, X. Fu, Y. Ma, F. Liu, M. Liu and H. Huang, *Small*, 2022, **18**, e2201695.
15 C. Liu, M. Zhang, J. Li, W. Xue, T. Zheng, C. Xia and J. Zeng, *Angew. Chem. Int. Ed. Engl.*, 2022, **61**, e202113498.
16 R. Yang, J. Duan, P. Dong, Q. Wen, M. Wu, Y. Liu, Y. Liu, H. Li and T. Zhai, *Angew. Chem. Int. Ed. Engl.*, 2022, **61**, e202116706.
17 X. Yan, C. Chen, Y. Wu, Y. Chen, J. Zhang, R. Feng, J. Zhang and B. Han, *Green Chem.*, 2022, **24**, 1989-1994.
18 H. Wu, J. Li, K. Qi, Y. Zhang, E. Petit, W. Wang, V. Flaud, N. Onofrio, B. Rebiere, L. Huang, C. Salameh, L. Lajaunie, P. Miele and D. Voiry, *Nat. Commun.*, 2021, **12**, 7210.
19 A. M. Asiri, J. Gao, S. B. Khan, K. A. Alamry, H. M. Marwani, M. S. J. Khan, W. A. Adeosun, S. M. Zakeeruddin, D. Ren and M. Gratzel, *J. Phys. Chem. Lett.*, 2022, **13**, 345-351.